Supplementary Information (SI) for ChemComm.
This journal is © The Royal Society of Chemistry 2025

-SUPPORTING INFORMATION-

Enzyme cascade reactions encapsulated in a liposome compartment with size-limited molecular transport

Shiwei Zhang,[a] Peng Lin,[a] Futa Komatsubara,[a] Eiji Nakata,[a] and Takashi Morii*[, a, b]

Contribution from [a]Institute of Advanced Energy, Kyoto University, Uji, Kyoto 611-0011, and [b]Department of Health and Nutrition, Kyoto Koka Women's University, Ukyo-ku, Kyoto 615-0882, Japan.

*To whom correspondence should be addressed:

Prof. Takashi Morii

Tel.: +81 75-325-5495

E-mail: morii.takashi.68s@st.kyoto-u.ac.jp

Table of contents

MATERIALS AND METHODS

Materials

M13 single-stranded viral DNA (p7308) was purchased from Guild Biosciences. BG-GLA-NHS (S9151S) and bovine serum albumin (BSA, BS9000S) were purchased from New England Biolabs. The pFN18A HaloTag® T7 Flexi® Vector and the 5-chlorohexane (CH) derivative [HaloTag Succinimidyl Ester (O2) Ligand (P1691)] were purchased from Promega. The purified DNA origami staple strands, oligonucleotide primers, and all other oligonucleotides were obtained from Sigma-Aldrich (St. Louis, MO), Japan Bio Services Co., Ltd. (Saitama, Japan), or Thermo Fisher Scientific (Tokyo, Japan). *Escherichia coli* (*E. coli*) BL21(DE3) competent cells were purchased from Thermo Fisher Scientific (Tokyo, Japan). *β*-Nicotinamide adenine dinucleotide in reduced (NADH) and oxidized (NAD^+) forms were obtained from Oriental Yeast (Tokyo, Japan). Xylose, xylitol and all other chemicals and reagents were purchased from Wako Chemicals (Tokyo, Japan) or Nacalai Tesque (Kyoto, Japan). The Mini Elute Gel Extraction Kit was from QIAGEN (Tokyo, Japan). The HisTrap HP column (5 mL), the HiTrap SP XL column (5 mL), and Sephacryl S-400 were purchased from GE Healthcare Japan Inc. (Tokyo, Japan). PrimeSTAR HS DNA polymerase, T4 DNA ligase, and *E. coli* DH5α competent cells were obtained from TaKaRa Bio Inc. (Shiga, Japan). Toyopearl HW-55F was purchased from Tosoh Corporation (Tokyo, Japan). The Ultrafree-MC-DV column was obtained from Merck Millipore (Darmstadt, Germany). The low-binding microtube (BT-150L, 1.5 mL, nonpyrogenic and RNase-/DNase-free) was purchased from Ina OPTIKA CO., Ltd. (Osaka, Japan). The COSMOSIL PBr packed column (4.6 mm i.d. × 150 mm) was purchased from Nacalai Tesque (Kyoto, Japan).

Expression of enzyme ZS-TeXR

Escherichia coli Rosetta(DE3)pLysS cells were transformed with pET30a/ZS-TeXR. The cells were cultured at 37 °C until the OD_{600} reached 0.6. Then, protein expression was induced with 1 mM IPTG for 12 hours at 25 °C. The soluble fraction of the collected cell lysate containing ZS-TeXR was loaded onto HisTrap HP column. The purified ZS-TeXR was dialyzed in a solution containing 20 mM phosphate buffer (pH 7.0), 100 mM NaCl, 5 mM β-mercaptoethanol (β-ME), and 50 % glycerol, then and stored at -20 °C. The amino acid sequence of ZS-TeXR ia shown

below. Fig. S1 shows an SDS-PAGE analysis of the purified ZS-TeXR.

Amino acid sequence of ZS-TeXR:

MMKTGEKRPYACPVESCDRRFSRSDELTRHIRIHTGQKPFQCRICMRNFSRSDHLTTHIRTHTG
EKPFACDICGRKFARSDERKRHTKIHTGEKEFGGSGGSDKDCEMKRTTLDSPLGKLELSGCEQG
LHEIIFLGKGTSAADAVEVPAPAAVLGGPEPLMQATAWLNAYFHQPEAIEEFPVPALHHPVFQQ
ESFTRQVLWKLLKVVKFGEVISYSHLAALAGNPAATAAVKTALSGNPVPILIPCHRVVQGDLDV
GGYEGGLAVKEWLLAHEGHRLGKPGLGGGSGGSMATPTIKLNSGYDMPLVGFGLWKVNRETCAD
QVYEAIKAGYRLFDGACDYGNEVEAGQGVARAIKEGIVKREDLFIVSKLWNTFHEADKVEPIAR
KQLADWGLDYFDLYLIHFPIALKYVDPAEIYPPGWTGTKKEVEFSNATIQETWQAMETLVDKKL
TRSIGISNFSAQLIMDLLRYARIRPATLQIEHHPYLTQQALVEYVQKEGIAVTAYSSFGPLSFL
ELGHQVAKDTPLLFEHSTVKSIAEKHGKTPAQVLLRWATQRNIAVIPRSDNPGRLAQNLDVTAW
DLEPADIEALSALNKNLRFNNPPSYGLYIPIFAGGSHHHHHH

Preparation of the DNA scaffold

A solution (50 µL) containing M13 p7308 (10 nM) and a mixture of staple DNA strands[1] (50 nM) in a buffer (pH 8.0) containing 5 mM Tris-HCl, 1 mM EDTA, 14 mM $MgCl_2$ was incubated at 80 °C for 5 min, cooled to 65 °C at 5 min/°C, incubated at 65 °C for 20 min, cooled to 25 °C at 20 min/°C, and then cooled to 4 °C using a C1000 Thermal Cycler (BioRad). The sample was then purified by gel filtration using an Ultrafree-MC-DV column to remove the excess staple strands. The DNA scaffold concentration was quantified by absorbance at 260 nm using Nanodrop (Thermo Fisher Scientific Inc.) and the determined extinction coefficient of the DNA scaffold (1.17×10^8 $M^{-1}cm^{-1}$).

Preparation of the DNA scaffold assembled with ZS-XR or HG-XDH

DNA scaffolds containing either the hairpin DNA binding sites with BG-GLA-NHS modification for ZS-TeXR attachment (Table S1) or 5-chlorohexane (CH) derivatives for HG-XDH attachment (Table S2) were constructed. A 20 nM DNA scaffold containing binding sites was incubated with 300 nM ZS-XR or HG-XDH in a buffer (pH 7.0) containing 40 mM Tris-HCl, 20 mM acetic acid, and 12.5 mM $MgCl_2$, 5 mM β-ME, 0.002% Tween20 and 1 µM $ZnCl_2$ at 4 °C overnight. The mixture was then purified by gel filtration using a 500 µL volume of Toyopearl

HW55F in an Ultrafree-MC-DV column with a buffer (pH 7.0) containing 40 mM Tris-HCl, 20 mM acetic acid, and 12.5 mM $MgCl_2$ to remove the excess unbound proteins from the mixture.

Estimation of the number of ZS-TeXR and HG-XDH per DNA origami skeleton

The ZS-TeXR and ODN-BG complex formed via covalent bonding of 100 nM ZS-TeXR and 1 μM ODN-BG in a 5 mM Tris buffer (pH 7.0) containing 12.5 mM $MgCl_2$, 0.002% Tween 20, 1 μM $ZnCl_2$, and 100 mM NaCl at 4 °C for 1 hour. Then, the complex was diluted from 100 nMof enzymes to 20, 30, 40, and 50 nM. The HG-XDH and ODN-CH complex was formed when the modular adaptor-fused HG-XDH (50 nM, dimer) reacted with the CH-modified ODN substrate (ODN-CH, 1 μM) in a 5 mM Tris buffer (pH 7.0) containing 12.5 mM $MgCl_2$, 0.002% Tween 20, 1 μM $ZnCl_2$, and 100 mM NaCl at 4 °C for 1 hour. Then, the complex was diluted from 100 nM of enzymes to 10, 20, 30, 40, and 50 nM. The free enzymes, complexes, and DNA origami assembled with enzymes were mixed with 1 x SDS loading buffer. The SDS-PAGE was stained with SYPRO Ruby Stain. Next, a standard curve was constructed to correlate concentration with the observed band intensity in the SDS-PAGE. Finally, the enzyme concentrations were determined by referencing the standard curve and the band intensity on the SDS-PAGE.

AFM imaging

The purified DNA nanostructure was deposited on a 1.5-mm in diameter mica surface, adsorbed for 5 min at ambient temperature, and then washed three times with a buffer (pH 8.0) containing 40 mM Tris-HCl, 20 mM acetic acid, and 14 mM $MgCl_2$. The sample was scanned in solution in tapping mode using a fast-scanning atomic force microscopy (AFM) system (Nano Live Vision, RIBM Co. Ltd., Tsukuba, Japan) with a silicon nitride cantilever (Olympus BL-AC10DS-A2). At least three independent samples were analyzed by AFM, and multiple images were taken from various areas of the mica surface.

TEM imaging

After removal of iodixanol through Amicon Ultra-0.5 mL Centrifugal Filters (30-kD NMWL), DNA scaffold (2.5 μL) was placed on a glow discharged TEM grid and incubated for 2 minutes. The excess sample was then removed with filter paper and incubated with 2% phosphotungstic acid (2.5 μL) for 2 minutes. Excess phosphotungstic acid was then removed with

filter paper. The samples were analyzed by using a TEM microscope (JEOL JEM-2200FS + CETCOR).

Preparation of liposome-coated WS-RD (LWS-RD)

A solution containing 7 nM WS-RD, 200 nM CF-modified DNA and 200 nM A647-modified DNA, 400 nM lipid-modified DNA, and 1% OG in 40 mM Tris-HCl (pH 7), 14 mM $MgCl_2$, 10 mM NaCl and 0.5 mM/2 mM/4 mM NADH was incubated at 30 °C for 1 hour. To form DNA-skeleton-guided liposomes, 75 μL of 5 mM DOPC was added to 150 μL of 5 nM lipids and CF- and A647-labeled WS-RD, bringing the total volume to 225 μL. The solution was then shaken for 30 minutes at room temperature. Then, the solution was diluted with 225 μL of a buffer containing 40 mM Tris-HCl (pH 7.0), 14 mM $MgCl_2$, 10 mM NaCl, and 0.5 mM, 2 mM, or 4 mM NADH, and 0.67% OG. The solution was dialyzed overnight against 2 L of this buffer containing 0.5 mM, 2 mM, or 4 mM NADH. Then, 190 μL of the recovered solution was mixed with 110 μL of 54% iodixanol in 1× hydration buffer and added to the bottom of a 11 × 34 mm centrifuge tube (Beckman Coulter Inc.). Then, six additional layers of 0 to 18% iodixanol in buffer were added to the centrifuge tube. The tube was spun in an MLA-130 rotor (Beckman Coulter Inc.) at 150,000 × g at 4 °C for 5 hours. The fractions (55 μL each) were collected. Each fraction was confirmed by agarose gel electrophoresis (Fig. S21). After collection, the buffer was exchanged using Amicon Ultra-0.5 mL Centrifugal Filters (30-kD).

Preparation of liposome-coated WS-RD containing OmpF (LWSO-RD)

According to the previous report[1], a 500 nM OmpF stock solution (prepared in 1% OG) was mixed 5 nM LWS-RD and incubated at 30 °C for 2 hours.

Fluorescence measurement to evaluate encapsulation efficiency

The fluorescence intensity of GelRed was measured at 25 °C using an Infinite 200 PRO microplate reader (TECAN, Austria, GmbH) with excitation at 490 nm and emission at 590 nm. WS, LWS, LWS-RD or LWSO-RD (1 nM) were added to a 96-well plate (90 μL) with GelRed (100 nM). After 15 minutes, 0.1% SDS was added to disrupt the liposomes.

Enzyme assay of ZS-TeXR, HG-XDH or cascade reaction

Enzyme assay of ZS-TeXR or cascade reaction

The catalytic activity of ZS-TeXR was analyzed by measuring the changes in absorbance at 340 nm (25 °C) due to the oxidation of NADH using an Infinite 200 PRO microplate reader (TECAN). In a typical experiment, a reaction (100 μL, 60 μL for 4 mM NADH) was initiated by adding 50 μL of ZS-TeXR (25 nM monomer, the concentration of WS-R is 4.9 nM, 5.1 molecules of ZS-TeXR were loaded per origami) to a 50 μL mixture containing 80 mM Tris-HCl (pH 7.0), 40 mM acetic acid, 25 mM $MgCl_2$, 1 mM, 4 mM, or 8 mM NADH, 800 mM xylose, 200 mM NaCl, 2 μM $ZnCl_2$, 10 μM BSA and 0.004% Tween 20. Enzyme activities were measured on a microplate (Greiner Microplate, 675301, 96-well, PS, F-bottom clear, chimney well, non-binding, half area) with 500 μM and 2 mM NADH. Enzyme activities with 4 mM NADH were measured on a full-area microplate.

Enzyme assay of HG-XDH

The catalytic activity of HG-XDH was measured by changes in absorbance at 340 nm (25 °C), derived from the production of NADH, using an Infinite 200 PRO microplate reader (TECAN). In a typical experiment, a reaction (100 μL) was initiated by adding 50 μL of HG-XDH (10 nM of monomer concentration, 5.3 nM WS-D, 1.9 HG-XDH dimer per origami) to a mixture of 50 μL containing 80 mM Tris-HCl (pH 7.0), 40 mM acetic acid, 25 mM $MgCl_2$, 4 mM NAD^+, 800 mM xylitol, 200 mM NaCl, 2 μM $ZnCl_2$, 10 μM BSA, and 0.004% Tween 20. Enzyme activities were measured on a microplate (Greiner Microplate, 675301, 96-well, PS, clear, medium-binding, half area).

Enzyme assay of cascade reaction (free TeXR-XDH, WS-RD and LWSO-RD)

The catalytic activity of the cascade reaction was analyzed by measuring changes in absorbance at 340 nm (25 °C), derived from the oxidation of NADH, using an Infinite 200 PRO microplate reader (TECAN). In a typical experiment (in bulk), a reaction (100 μL, 60 μL for 4 mM NADH) was initiated by an adding 50 μL of free TeXR-XDH, WS-RD (5 nM WS-RD, 25 nM TeXR monomer and 10 nM XDH dimer) to a mixture (50 μL) containing 80 mM Tris-HCl (pH

7.0), 40 mM acetic acid, 25 mM $MgCl_2$, 1 mM, 4 mM, or 8 mM NADH, 800 mM xylose, 200 mM NaCl, 2 μM $ZnCl_2$, 10 μM BSA, and 0.004% Tween 20. For the LWSO-RD reaction, a reaction (100 μL, 60 μL for 4 mM NADH) was initiated by an adding 50 μL LWSO-RD containing 500 μM, 2 mM, or 4 mM NADH (5 nM LWSO-RD, 25 nM TeXR monomer and 10 nM XDH dimer) to a mixture (50 μL) containing 80 mM Tris-HCl (pH 7.0), 40 mM acetic acid, 25 mM $MgCl_2$, 800 mM xylose, 200 mM NaCl, 2 μM $ZnCl_2$, 10 μM BSA, and 0.004% Tween 20. For the control experiment, a reaction (100 μL, 60 μL for 4 mM NADH) was initiated by adding 50 μL free TeXR-XDH, WS-RD containing 0.35 μM, 1.3 μM, or 2.7 μM NADH (5 nM WS-RD, 25 nM TeXR monomer and 10 nM XDH dimer) to a mixture (50 μL) containing 80 mM Tris-HCl (pH 7.0), 40 mM acetic acid, 25 mM $MgCl_2$, 800 mM xylose, 200 mM NaCl, 2 μM $ZnCl_2$, 10 μM BSA, and 0.004% Tween 20. Enzyme activities were measured on the microplate (Greiner Microplate, 675301, 96-well, PS, F-bottom, chimney well, clear, non-binding, half area) with 500 μM and 2 mM NADH. Enzyme activities with 4 mM NADH were measured on a full-area microplate.

Coupled enzyme assay using xylulose kinase (XK) and HPLC quantification

Xylulose kinase fused to AZP4 and a CLIP-tag (AC-XK) was used for the coupled reaction to quantify xylulose. An enzyme reaction solution (80 μL, XDH) was mixed with 500 nM AC-XK in a buffer (pH 7.0) containing 40 mM Tris-HCl, 20 mM acetic acid, 12.5 mM $MgCl_2$, 1 mM DTT, 1 μM $ZnCl_2$, 0.002% Tween 20, 100 mM NaCl, and 1 mM ATP. The mixture was incubated at 25°C for 1 hour. The total volume was 100 μL. The enzyme reactions were quenched by heating at 60 ℃ for 1 minute. The enzyme cascade reactions were monitored by HPLC at 260 nm. HPLC conditions: COSMOSIL PBr-packed column (4.6 mm i.d. × 150 mm); eluent A: 20 mM phosphate buffer (pH 7.0); eluent B: 40% methanol in 20 mM phosphate buffer (pH 7.0); gradient of eluent B increased from 0% to 100% over 30 minutes at a flow rate of 1 mL/min.

Estimation the effective NADH concentration in the bulk solution

In a typical solution (100 μL), the concentration of LWSO-RD is 5 nM, and its diameter is 75 nm. The number of LWSO-RD particles (*N*) is calculated using the formula:

$$N = 6.02 \text{ x } 10^{23}\,\text{mol}^{-1} \text{ x } 5 \text{ x } 10^{-9}\,\text{mol/L} \text{ x } 1 \text{ x } 10^{-4}\,\text{L} = 3 \text{ x } 10^{11}$$

The volume of a single LWSO-RD particle is calculated using the formula for the volume of a sphere:

$$V_{\text{LWSO-RD}} = 4/3\ \pi(37.5\ \text{nm})^3 = 2.2 \text{ x } 10^5\ \text{nm}^3$$

The total volume of all LWSO-RD particles is:

$$V_{\text{total-LWSO-RD}} = N\text{x}\ V_{\text{LWSO-RD}} = 6.6\text{x } 10^{16}\ \text{nm}^3$$

The ratio of the total volume of LWSO-RD particles to the volume of the solution is:

$$V_{\text{total-Lipo-WS}}/\ V_{\text{solution}} = 6.6 \text{ x } 10^{-4} = 0.066\%$$

The effective NADH concentration in the bulk solution:

$$C_{\text{effective NADH}} = 6.6 \text{ x } 10^{-4}\ C_{\text{LWSO-RD-NADH}} = 6.6 \text{ x } 10^{-4} \text{ x } 4\ \text{mM} = 2.7\ \mu\text{M}$$

Estimation the NADH regeneration of enzyme cascade ZS-TeXR/HG-XDH

The cascade reaction was first evaluated by monitoring the time-dependent change in NADH concentration based on the absorbance at 340 nm. To further quantify the regenerated NADH in the TeXR/XDH enzyme cascade, the reaction was coupled with XK, which converts xylulose (the product of the XDH reaction) into xylulose-5-phosphate by consuming an equimolar amount of ATP. During this process, ATP is simultaneously converted into ADP. Because the formation of xylulose-5-phosphate and the conversion of ATP to ADP occurs in a 1:1 stoichiometric ratio with NADH regeneration, the amount of regenerated NADH can be indirectly determined from the concentration of ADP produced in the coupled XK reaction (Fig. 4a). Therefore, the XK reaction was employed to couple with the TeXR/XDH cascade to quantitatively evaluate NADH regeneration.

After the cascade reaction, an enzyme reaction solution (80 μL, TeXR/XDH) was mixed with 500 nM AC-XK in a 20 μL buffer (pH 7.0) containing 40 mM Tris-HCl, 20 mM acetic acid, 12.5 mM $MgCl_2$, 1 mM DTT, 1 μM $ZnCl_2$, 0.002% Tween 20, 100 mM NaCl, and 1 mM ATP. The mixture was incubated at 25°C for 1 hour. The total volume was 100 μL. The enzyme reactions were quenched by heating at 60 ℃ for 1 minute. The enzyme cascade reactions were monitored by HPLC at 260 nm. HPLC conditions: COSMOSIL PBr-packed column (4.6 mm i.d. × 150 mm); eluent A: 20 mM phosphate buffer (pH 7.0); eluent B: 40% methanol in 20 mM phosphate buffer (pH 7.0); gradient of eluent B increased from 0% to 100% over 30 minutes at a flow rate of 1 mL/min.

Table S1. Nucleotide sequences for the staple strands containing the binding sites for ZS-TeXR with BG modification.

Oligo DNA	Sequence (from 5' to 3')
i6-ZF	TTTAATGTGCGGCCTCAGGA CTTACGCCCACGCGCGTT^{BG}TTCGCGCGTGGGCGTAAG AGATCGCATGGCTAAAACATC
a6-ZF	CAGGCGAACAGGTGCCGTAA CTTACGCCCACGCGCGTT^{BG}TTCGCGCGTGGGCGTAAG AGCACTATGGTTTGCCCGAGA
j6-ZF	GTACAGACACAGAGCCACCA CTTACGCCCACGCGCGTT^{BG}TTCGCGCGTGGGCGTAAG CCCTCAGACAGATGTGACCTT
e7-ZF	TATAAGTACACGCTAACGAG CTTACGCCCACGCGCGTT^{BG}TTCGCGCGTGGGCGTAAG CGTCTTTTCGAGAGATCACCG
g7-ZF	GATTTAGGTTAAAGGCCGCT CTTACGCCCACGCGCGTT^{BG}TTCGCGCGTGGGCGTAAG TTTGCGGTAATACAACAATTC
k7-ZF	ACCCAAAAAAGCCCCAAAAA CTTACGCCCACGCGCGTT^{BG}TTCGCGCGTGGGCGTAAG CAGGAAGATAATAAACTCCTT

Note: BG modified amino-C6-T was denoted as T^{BG}

Table S2. Nucleotide sequences for the staple strands containing the binding sites for HG-XDH with CH modification.

Oligo DNA	Sequence (from 5' to 3')
a7-AP1	AGGTCAGAAATCCTGTTTGA GT^{CH}TCATGAGTCATGAGTTTTCT^{CH}CATGACTCATGAAC TGGTGGTAGGAGGTCACAAAC
i7-AP1	AAATTTTCGGAAGGTTATCT GT^{CH}TCATGAGTCATGAGTTTTCT^{CH}CATGACTCATGAAC AAAATATTAAAATTTTTAACC

Note: CH modified amino-C6-T was denoted as T^{CH}

Table S3. Equations to estimate the concentration (x-axis) of ATP and ADP from the peak area (y-axis) in Fig. S13.

	ATP (peak area)	**ADP (peak area)**	**NAD^+ (peak area)**	**NADH (peak area)**
Equation	y = 129397.21 + 89749.96 *x	y = 69797.26 + 81956.42 *x	y = 778384.06 + 98852.71 *x	y = -38497.09 + 80264.15848 *x
R-Square	0.99997	0.99999	0.9988	0.99996

Table S4. The amount of initial NADH in the bulk solution (100 μL) was estimated from the peak area in HPLC**.**

	Concentration in bulk solution (μM)
500 μM NADH in LWSO-RD (5 μM)	1.01 ± 0.34
2 mM NADH in LWSO-RD (5 μM)	1.65 ± 0.47
4 mM NADH in LWSO-RD (5 μM)	2.08 ± 0.35

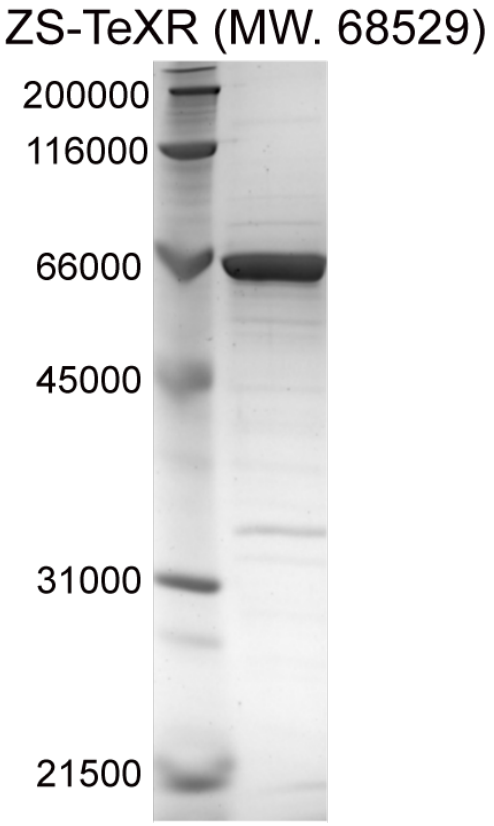

Figure S1. An SDS-PAGE analysis of the purified ZS-TeXR.

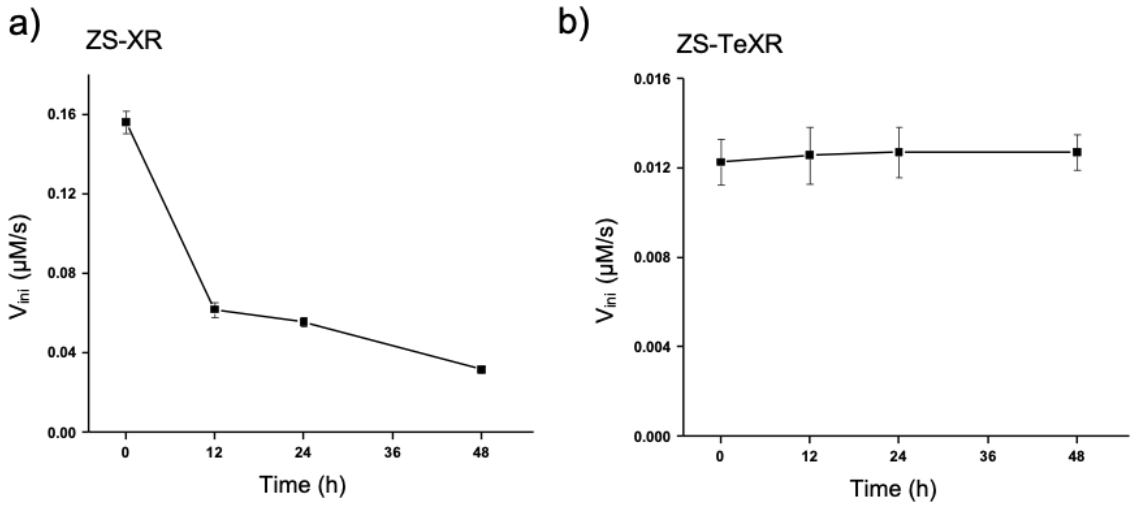

Figure S2. Schematic of the 100 nM ZS-XR and ZS-TeXR enzyme reaction. (a) Comparison of the initial reaction velocity of free ZS-XR at different incubation times. (b) Comparison of the initial reaction velocity of free ZS-TeXR at different incubation times.

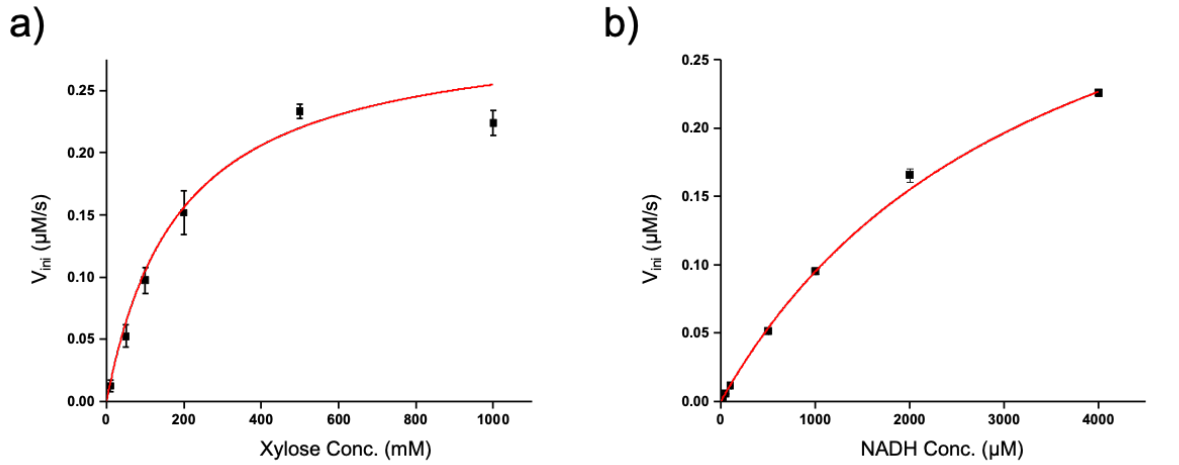

Xylose	
V_{max} (μM/s)	0.303 ± 0.027
K_m (mM)	187.89 ± 53.51
K_{cat} (min^{-1})	36.4 ± 1.8
K_{cat}/K_m ($min^{-1}mM^{-1}$)	0.194 ± 0.034
R-Square (COD)	0.98873

NADH	
V_{max} (μM/s)	0.383 ± 0.005
K_m (mM)	3.15 ± 0.064
K_{cat} (min^{-1})	46.2 ± 0.6
K_{cat}/K_m ($min^{-1}mM^{-1}$)	14.67 ± 0.9
R-Square (COD)	0.99913

Figure S3. Michaelis-Menten kinetics for the ZS-TeXR reaction. (a) Variations in ZS-TeXR activity with xylose concentration from 0 to 1000 mM. (b) Variations in ZS-TeXR activity with increasing concentrations of NADH from 0 to 4 mM.

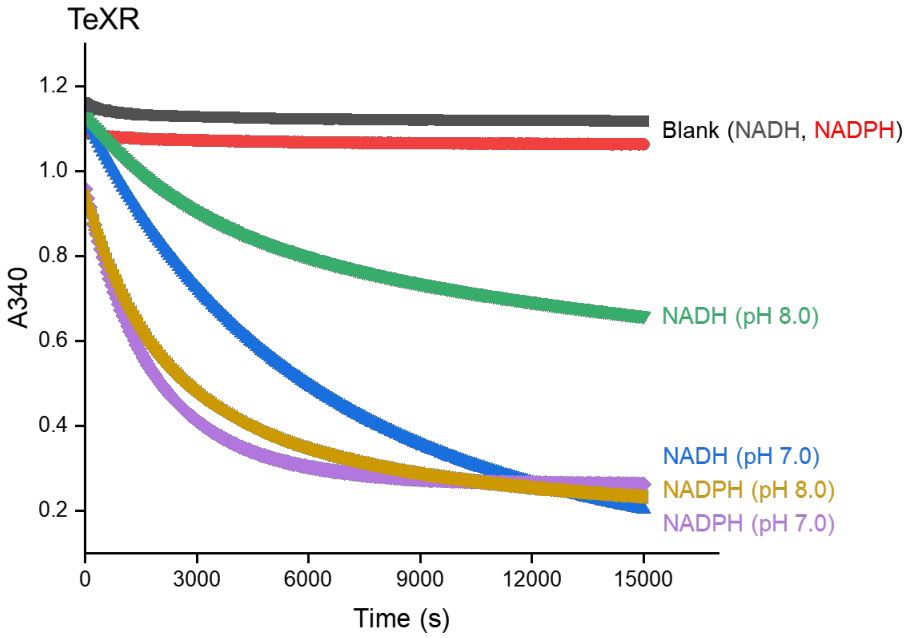

Figure S4. The time course of the A340 of the ZS-TeXR reaction was measured at pH 7.0 or pH 8.0 with either NADH or NADPH as the cofactor. The enzyme reactions were carried out using 100 nM ZS-TeXR that react with 400 mM xylose and 500 µM either NADH or NADPH in a 5 mM Tris buffer (pH 7.0 or pH 8.0) which contained 12.5 mM $MgCl_2$, 5 µM BSA, 0.002% Tween 20, 1 µM $ZnCl_2$, and 100 mM NaCl at 25 °C.

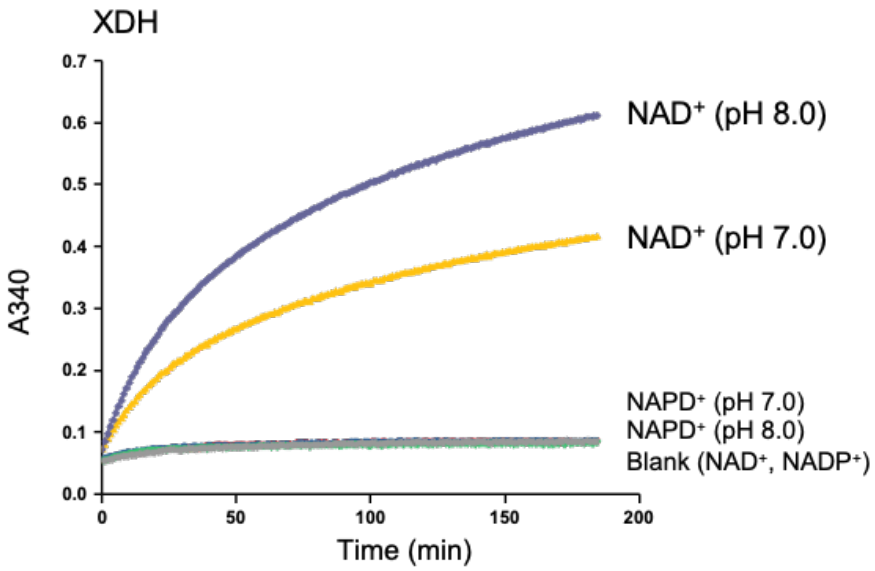

Figure S5. The time course of the A340 of the HG-XDH reaction was measured at pH 7.0 with either NAD^+ or $NADP^+$ as the cofactor. The enzyme reactions were carried out using 10 nM HG-XDH that react with 400 mM xylitol and 500 µM either NAD^+ or $NADP^+$ in a 5 mM Tris buffer (pH 7.0 or pH 8.0) containing 12.5 mM $MgCl_2$, 5 µM BSA, 0.002% Tween 20, 1 µM $ZnCl_2$, and 100 mM NaCl at 25 °C.

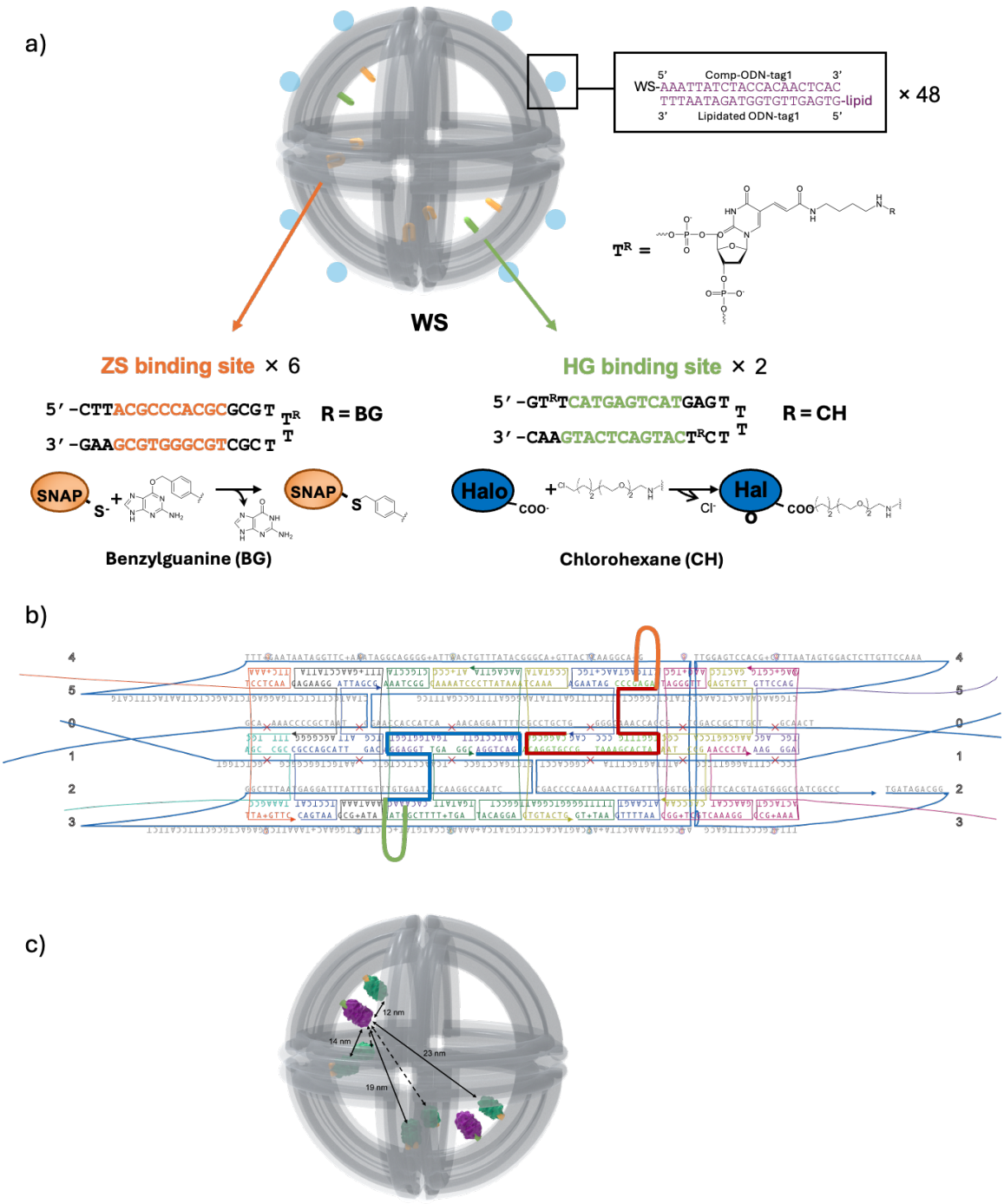

Figure S6. (a) A scheme presents 6 binding sites for ZS-TeXR and 2 for HG-XDH, which are assembled on a DNA scaffold. It contains Zif268 binding site and a SNAP-tag that reacts with its substrate, benzylguanine (BG), and the GCN4 binding site and a Halo-tag that reacts with its substrate, chlorohexane (CH). (b) A detailed scheme showing the positions of ZS binding site and HG binding sites. (c) The average inter-enzyme distance was estimated to be 16.8 nm.

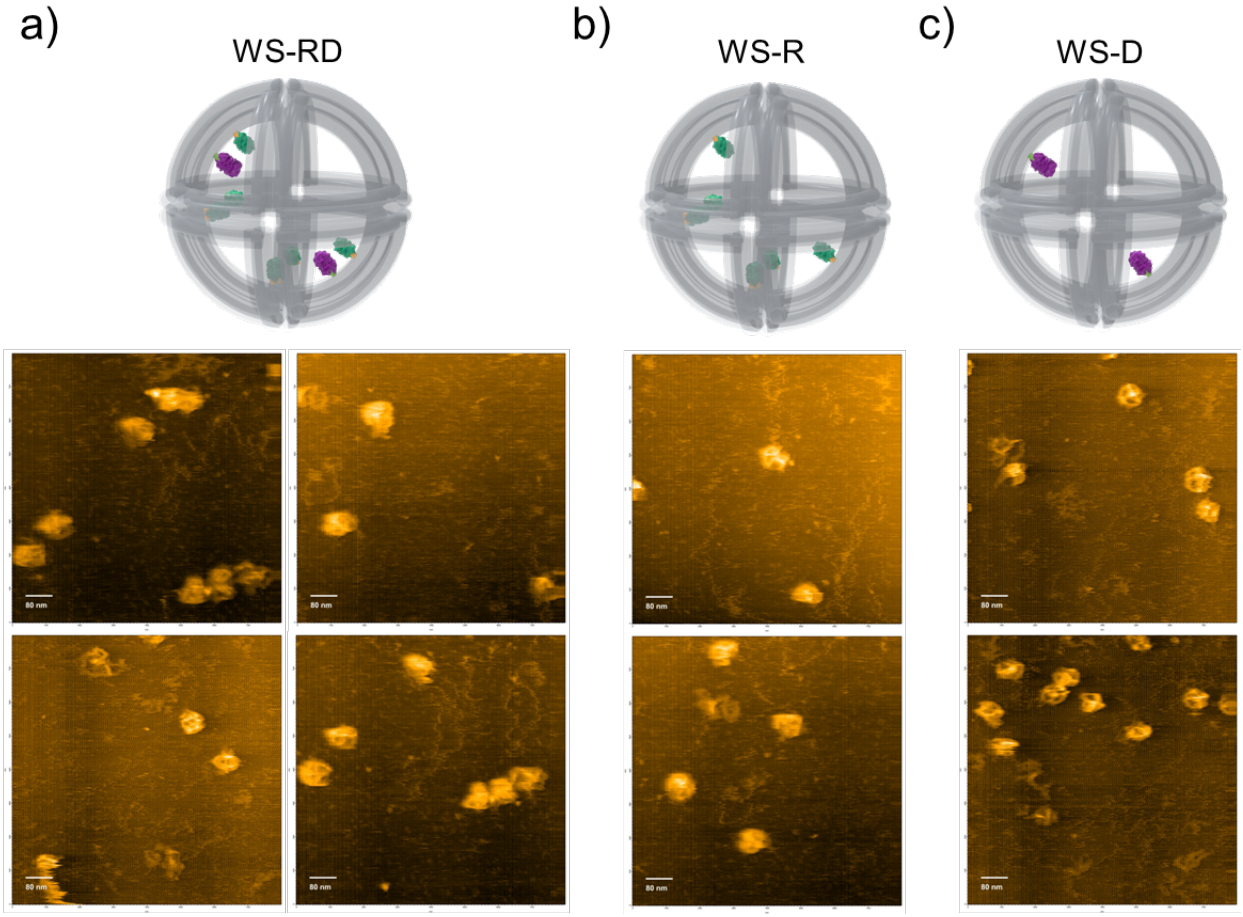

Figure S7. AFM images of (a) WS-RD, (b) WS-R, and (c) WS-D. Scale bar: 80 nm.

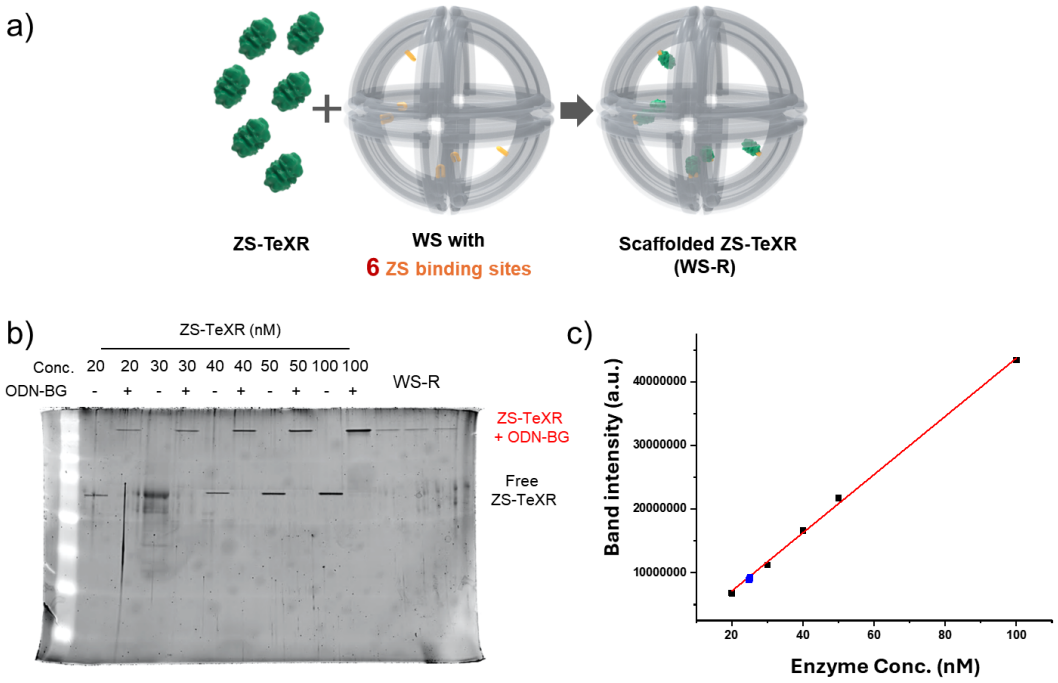

Figure S8. (a) Scheme illustrating the construction of WS-R. (b) SDS-PAGE analysis estimating the amount of ZS-TeXR on the WS-R DNA origami skeleton. The ZS-TeXR concentration was measured by band intensity. (c) The standard curve was estimated by quantifying the slower-migrating band, indicating the formation of a covalent complex between ZS-TeXR and ODN-BG. The enzyme concentrations are 20, 30, 40, and 50 nM. The blue dots represent the ZS-TeXR enzyme concentration on the DNA origami skeleton, which are estimated based on the standard curve.

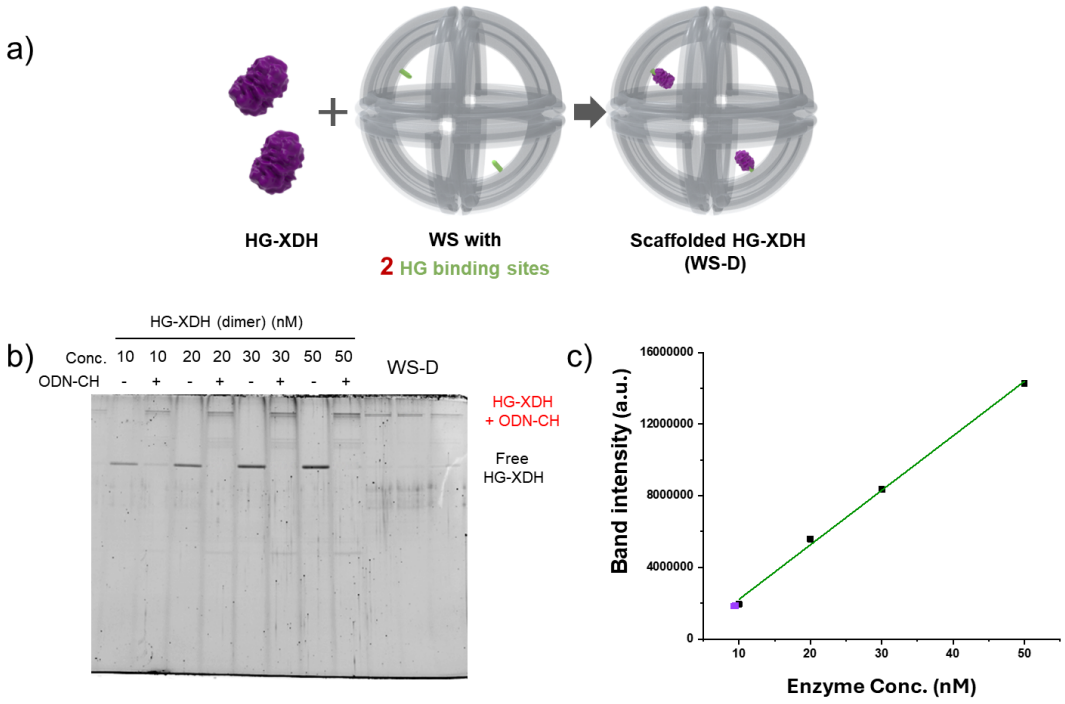

Figure S9. (a) Scheme illustrating the construction of WS-D. (b) SDS-PAGE analysis estimating the amount of HG-XDH on the WS- X DNA origami skeleton. The HG-XDH concentration was measured by band intensity. (c) The standard curve was estimated by quantifying the slower-migrating band, indicating the formation of a covalent complex between HG-XDH and ODN-CH. The enzyme concentrations are 10, 20, 30, and 50 nM. The purple dots represent the HG-XDH enzyme concentration on the DNA origami skeleton, which are estimated based on the standard curve.

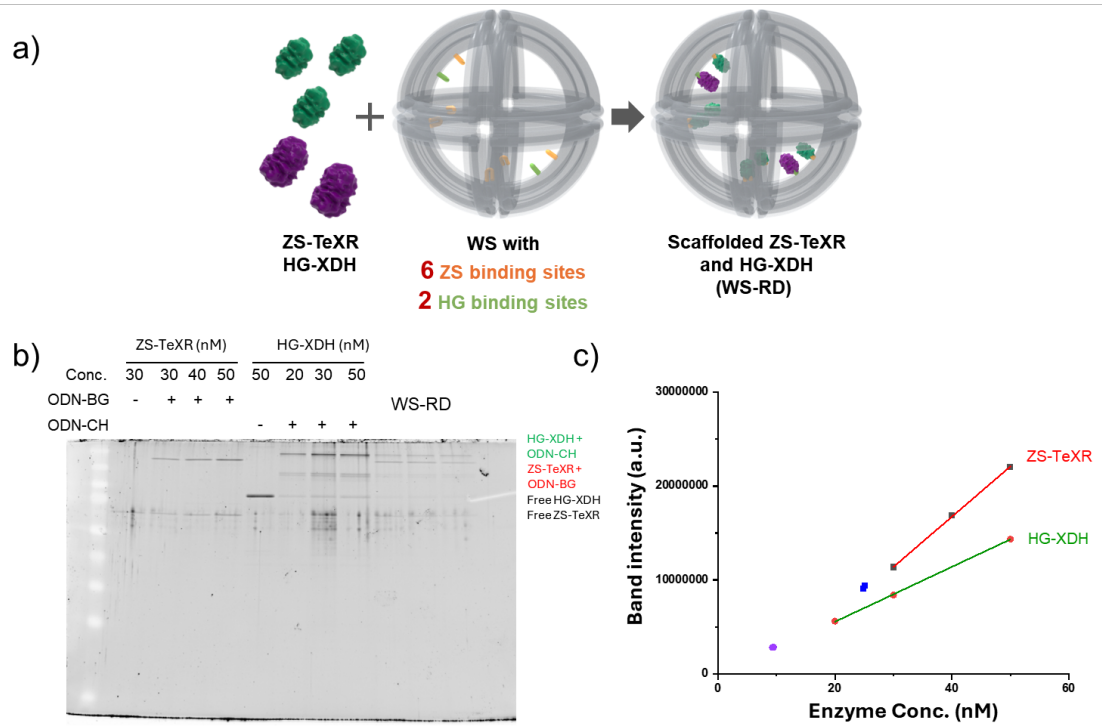

Figure S10. (a) Scheme illustrating the construction of WS-RD. (b) SDS-PAGE analysis estimating the amount of co-assembled ZS-TeXR and HG-XDH on the WS-RD DNA origami skeleton. The ZS-TeXR and HG-XDH concentrations were measured by band intensity. (c) The standard curve was estimated by quantifying the slower-migrating band, indicating the formation of a covalent complex between ZS-TeXR and ODN-BG or between HG-XDH and ODN-CH. The ZS-TeXR concentrations (red) are 30, 40, and 50 nM. The HG-XDH (green) concentrations are 20, 30, and 50 nM. The blue dots represent the ZS-TeXR enzyme concentration on the DNA origami skeleton, which are estimated based on the standard curve. The purple dots represent the HG-XDH enzyme concentration on the DNA origami skeleton, which are estimated based on the standard curve.

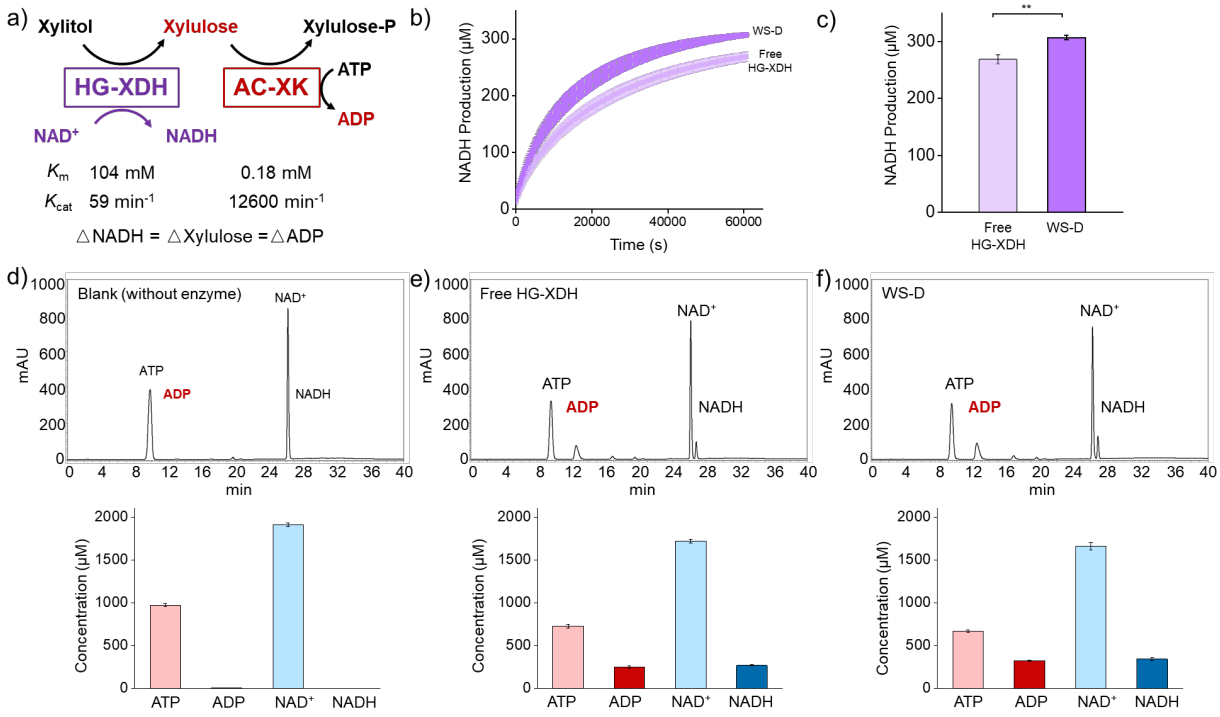

Figure S11. (a) A schematic diagram illustrates the cascade reaction involving HG-XDH and AC-XK. The kinetic parameters, K_m and K_{cat}, are shown below each enzyme to provide a quantitative overview of their catalytic efficiency and substrate affinity in the cascade system. (b) The time course of the NADH production in the reactions. (c) NADH production by Free HG-XDH (10 nM) and WS-D (5 nM, 10 nM HG-XDH) after the reaction was allowed to proceed for 10 hours and then quenched. To verify the reliability of this method, the NADH yield from the HG-XDH reaction with xylitol and NAD^+ was compared with the ADP yield from treating the XDH reaction mixture with XK and ATP. The HG-XDH reaction in bulk solution (free HG-XDH) and the reaction assembled on WS with two HG binding sites (WS-D) were analyzed by monitoring the absorbance of NADH production at 340 nm (Fig. 3a). The NADH production by free HG-XDH and WS-D was measured after the reaction proceeded for 10 hours and was quenched. Reactions with free HG-XDH and WS-D produced 268.1 ± 8.2 μM and 313.1 ± 4.2 μM of NADH, respectively. Asterisks indicate significant difference between groups (**$p < 0.01$). (d) HPLC chromatograms of the reaction products and ADP production (μM) by Blank (without enzyme) after 10 hours. The coupled reaction of HG-XDH and AC-XK was analyzed by high-performance liquid

chromatography (HPLC) to quantify the amount of ADP generated after treating the reaction mixture for 10 hours and then quenched by heating at 60 °C for one minute. (e, f) Reactions with (e) free HG-XDH (10 nM) and (f) WS-D (5 μM, 10 nM HG-ZDH) produced 269.1 ± 7.4 μM and 343.6 ± 20.5 μM of NADH, respectively, which is consistent with the results in Fig. S11c. These ADP and NADH yields indicate that the yield of the AC-XK reaction is greater than 93%. Therefore, AC-XK can be used to reasonably estimate the efficiency of the TeXR/XDH cascade reaction. The amounts of NADH and ADP in each reaction mixture were estimated from the peak areas using the calibration curves (Fig. S12).

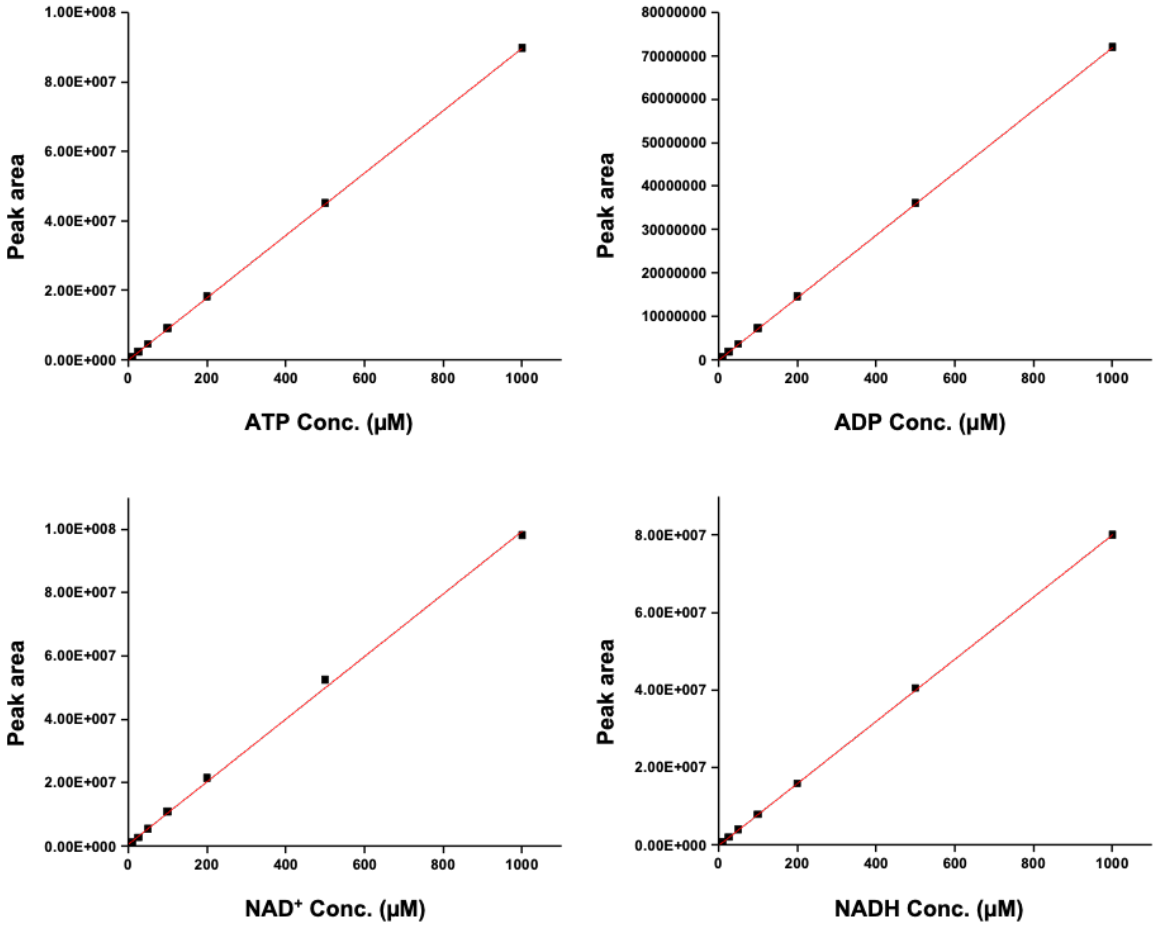

Figure S12. The standard curve for estimating the ATP and ADP concentration from the HPLC peak area of ATP and ADP. The amounts of NADH and ADP in each reaction mixture were estimated from the peak areas using the calibration curves.

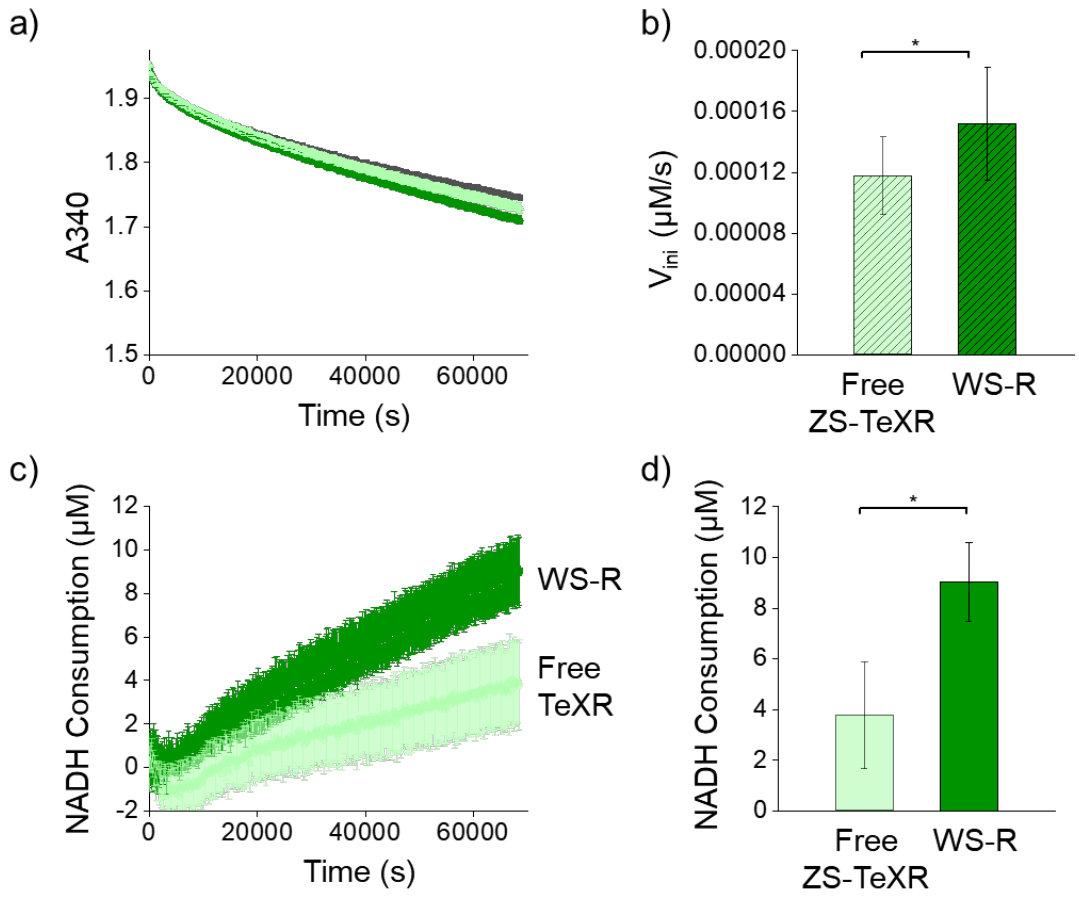

Figure S13. (a) The time course of the Free ZS-TeXR (25 nM) and WS-R (5 nM) reactions with 500 μM NADH was monitored by A340. (b) The initial velocity of the Free ZS-TeXR and WS-R reactions was calculated from the data collected between 0 and 2000 seconds. Asterisks indicate significant difference between groups (*$p < 0.05$). (c) The time course of NADH consumption in the reactions. (d) NADH consumption by Free TeXR and WS-R after the reaction was allowed to proceed for 10 hours and then quenched. Asterisks indicate significant difference between groups (*$p < 0.05$).

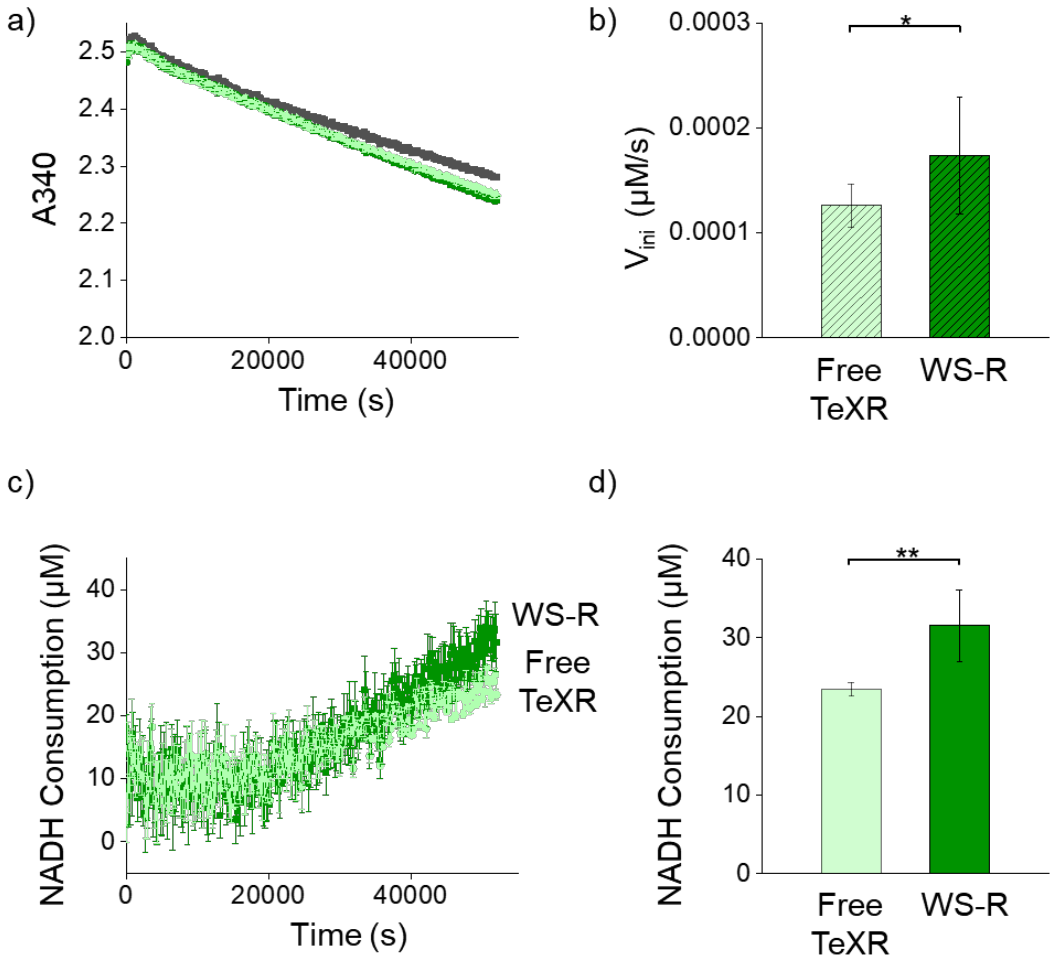

Figure S14. (a) The time course of the Free ZS-TeXR and WS-R reactions with 2 mM NADH was monitored by A340. (b) The initial velocity of the Free ZS-TeXR and WS-R reactions was calculated from the data collected between 0 and 2000 seconds. Asterisks indicate significant difference between groups (*$p < 0.05$). (c) The time course of NADH consumption in the reactions. (d) NADH consumption by Free TeXR and WS-R after the reaction was allowed to proceed for 10 hours and then quenched. Asterisks indicate significant difference between groups (*$p < 0.05$).

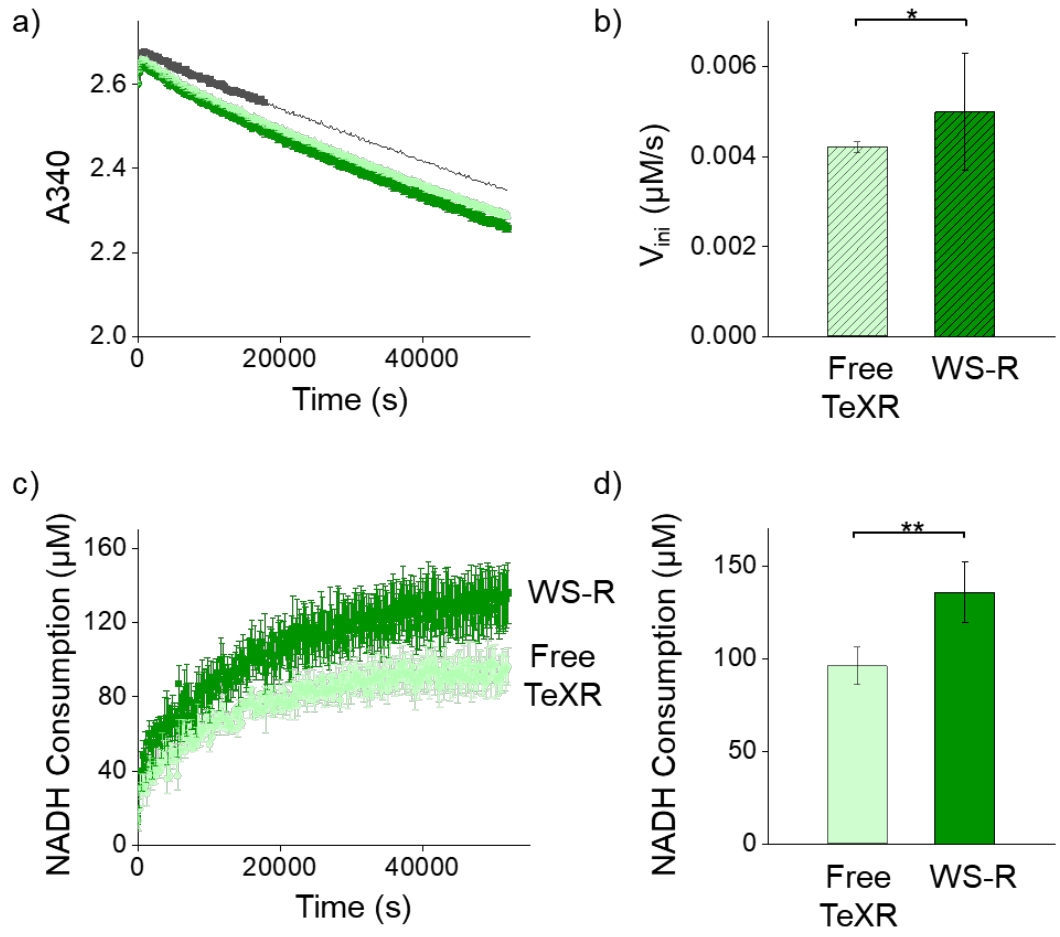

Figure S15. (a) The time course of the Free ZS-TeXR and WS-R reactions with 4 mM NADH was monitored by A340. (b) The initial velocity of Free ZS-TeXR (25 nM) and WS-R (5 nM) reactions was calculated from the data collected between 0 and 2000 seconds. Asterisks indicate significant difference between groups (*$p < 0.05$). (c) The time course of NADH consumption in the reactions. (d) NADH consumption by Free TeXR and WS-R after the reaction was allowed to proceed for 10 hours and then quenched. Asterisks indicate significant difference between groups (**$p < 0.01$).

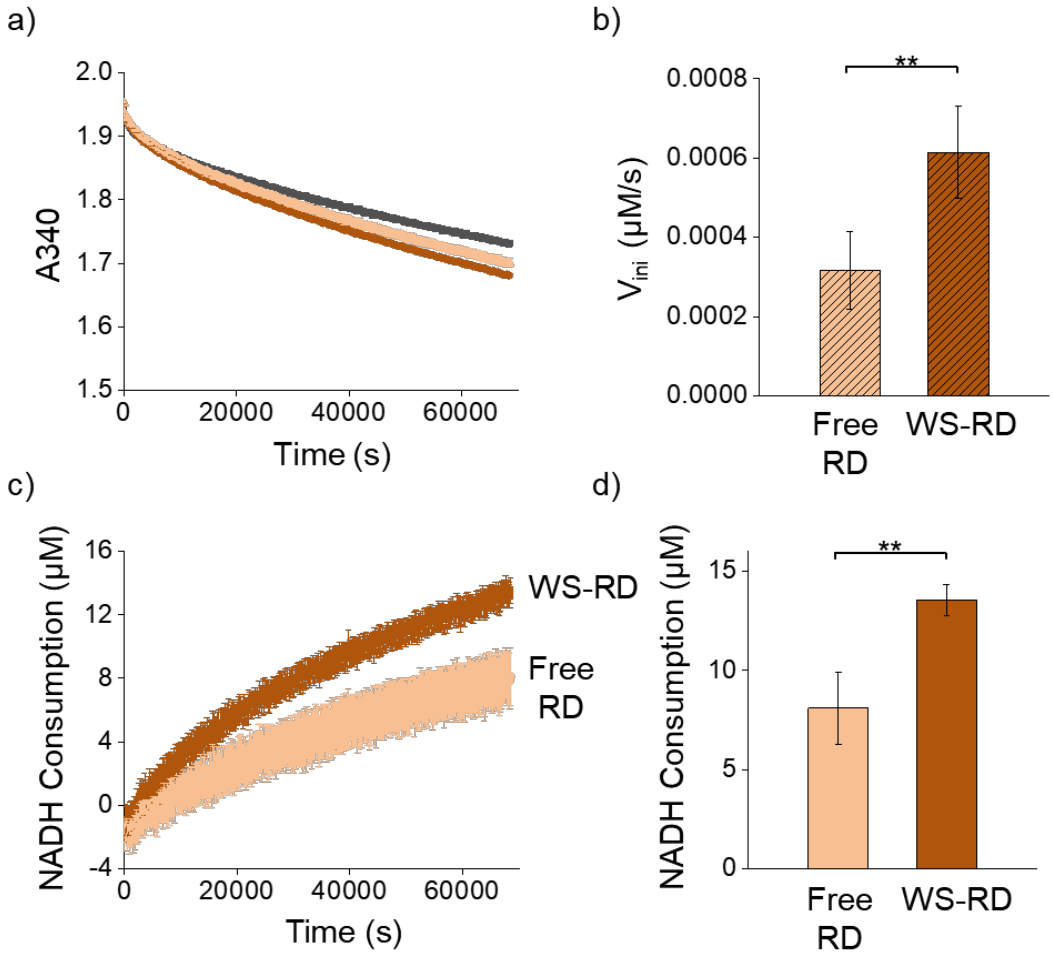

Figure S16. (a) The time course of the Free TeXR-XDH and WS-RD reactions with 500 μM NADH was monitored by A340. (b) The initial velocity of Free TeXR/XDH (25 nM/10 nM) and WS-RD (5 nM) reactions was calculated from the data collected between 0 and 2000 seconds. Asterisks indicate significant difference between groups (**$p < 0.01$). (c) The time course of NADH consumption in the reactions. (d) NADH consumption by Free TeXR/XDH and WS-RD after the reaction was allowed to proceed for 10 hours and then quenched. Asterisks indicate significant difference between groups (**$p < 0.01$).

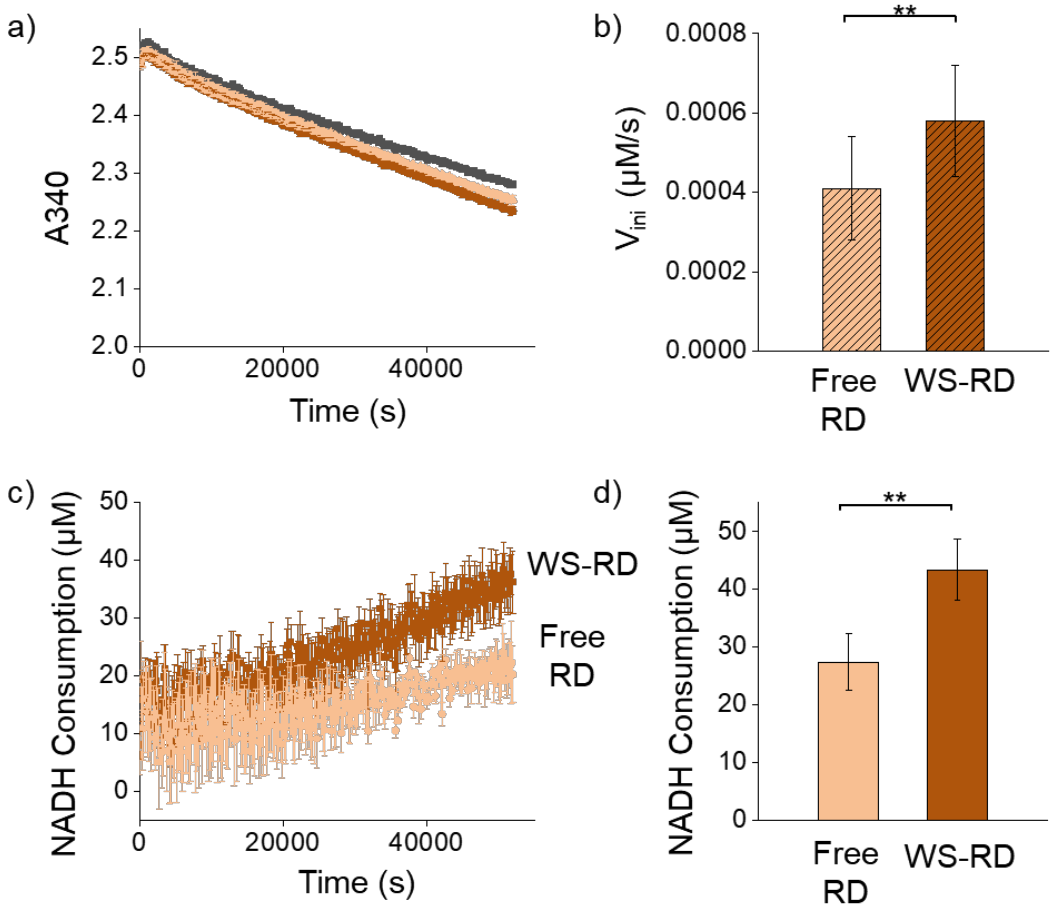

Figure S17. (a) The time course of the Free TeXR-XDH and WS-RD reactions with 2 mM NADH monitored by A340. (b) The initial velocity of Free TeXR/XDH (25 nM/10 nM) and WS-RD (5 nM) reactions was calculated from the data collected between 0 and 2000 seconds. Asterisks indicate significant difference between groups (**$p < 0.01$). (c) The time course of NADH consumption in the reactions. (d) NADH consumption by Free TeXR-XDH and WS-RD after the reaction was allowed to proceed for 10 hours and then quenched. Asterisks indicate significant difference between groups (**$p < 0.01$).

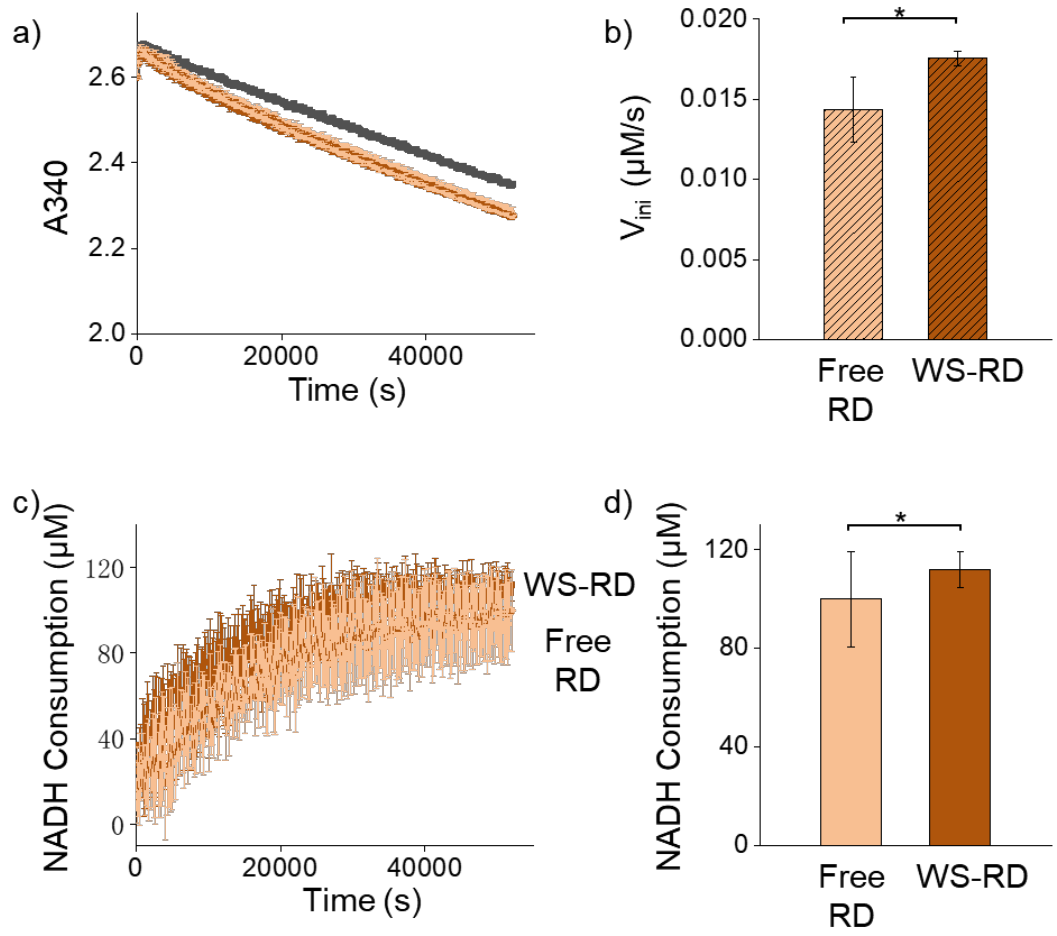

Figure S18. (a) The time course of the Free TeXR-XDH and WS-RD reactions with 4 mM was monitored by A340. (b) The initial velocity of Free TeXR/XDH (25 nM/10 nM) and WS-RD (5 nM) reactions was calculated from the data collected between 0 and 2000 seconds. Asterisks indicate significant difference between groups (*$p < 0.05$). (c) The time course of the NADH consumption in the reactions. (d) NADH consumption by Free TeXR-XDH and WS-RD after the reaction was allowed to proceed for 10 hours and then quenched. Asterisks indicate significant difference between groups (*$p < 0.05$).

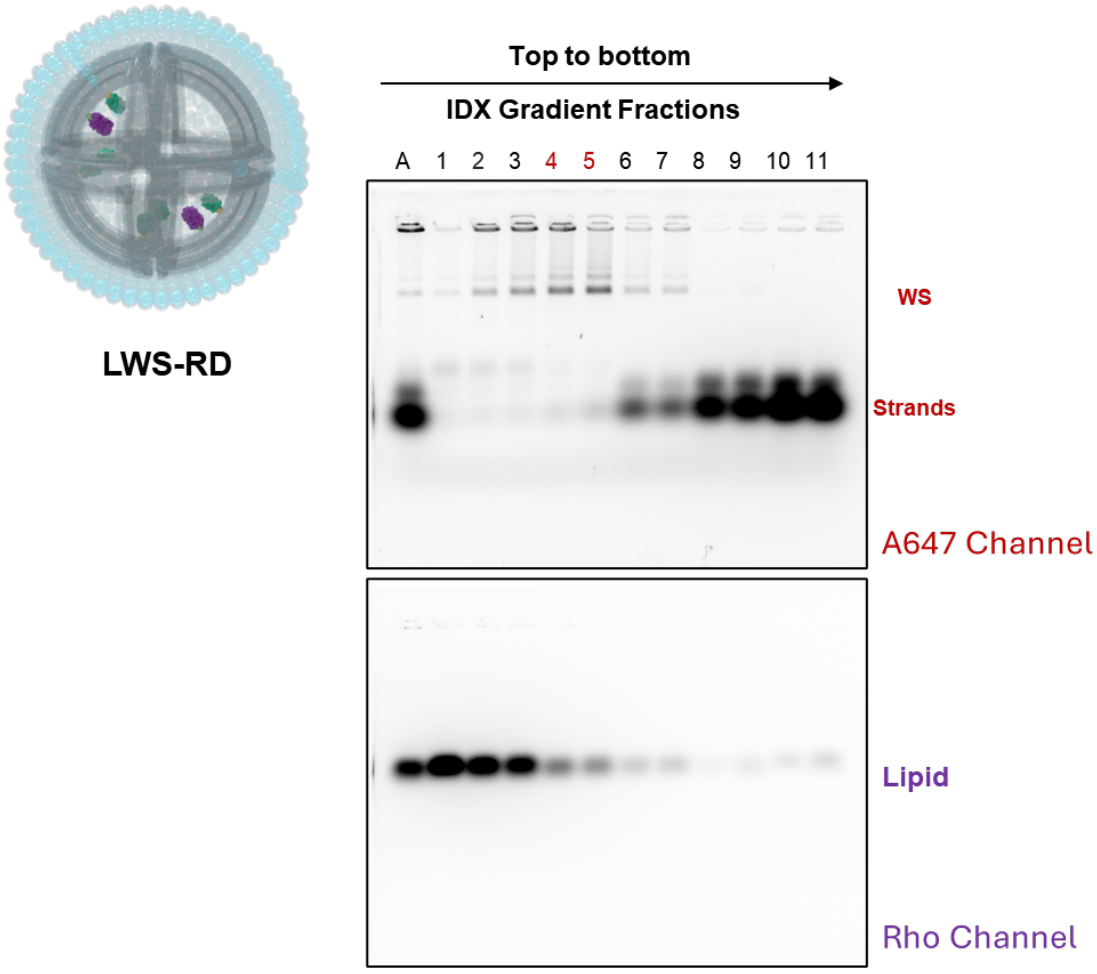

Figure S19. Agarose gel images of the density gradient fractions of LWS-RD. The fractions are numbered sequentially from F1 to F11 from the top to the bottom of the gradient. Lane A: the sample before purification. Fractions 4 and 5 were collected for further experimentation.

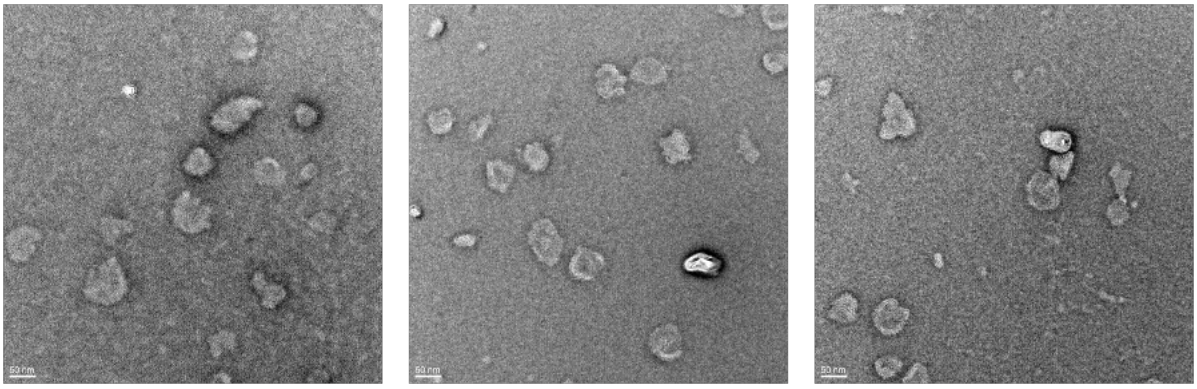

Figure S20. TEM images of LWSO-RD. Scale bar: 50 nm.

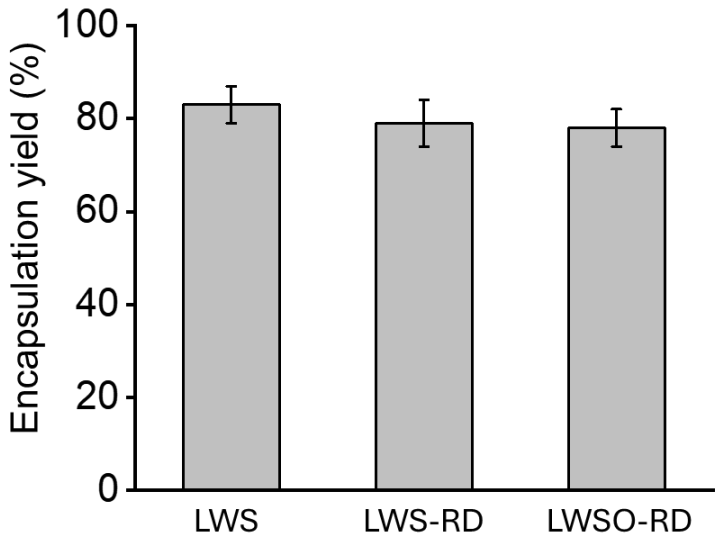

Figure S21. The encapsulation yields of LWS, LWS-RD, and LWSO-RD were estimated using GelRed. All encapsulation experiments in this study were performed using multiple independently prepared batches of DNA origami, proteins, and liposomes. Using our previously established protocol (Supplementary References 1 and 2), the encapsulation efficiencies of LWS, LWS-RD, and LWSO-RD were quantified as 83 ± 4%, 79 ± 5%, and 78 ± 4%, respectively. These values were consistent across independent preparations and exhibited only minor variation (typically <5%).

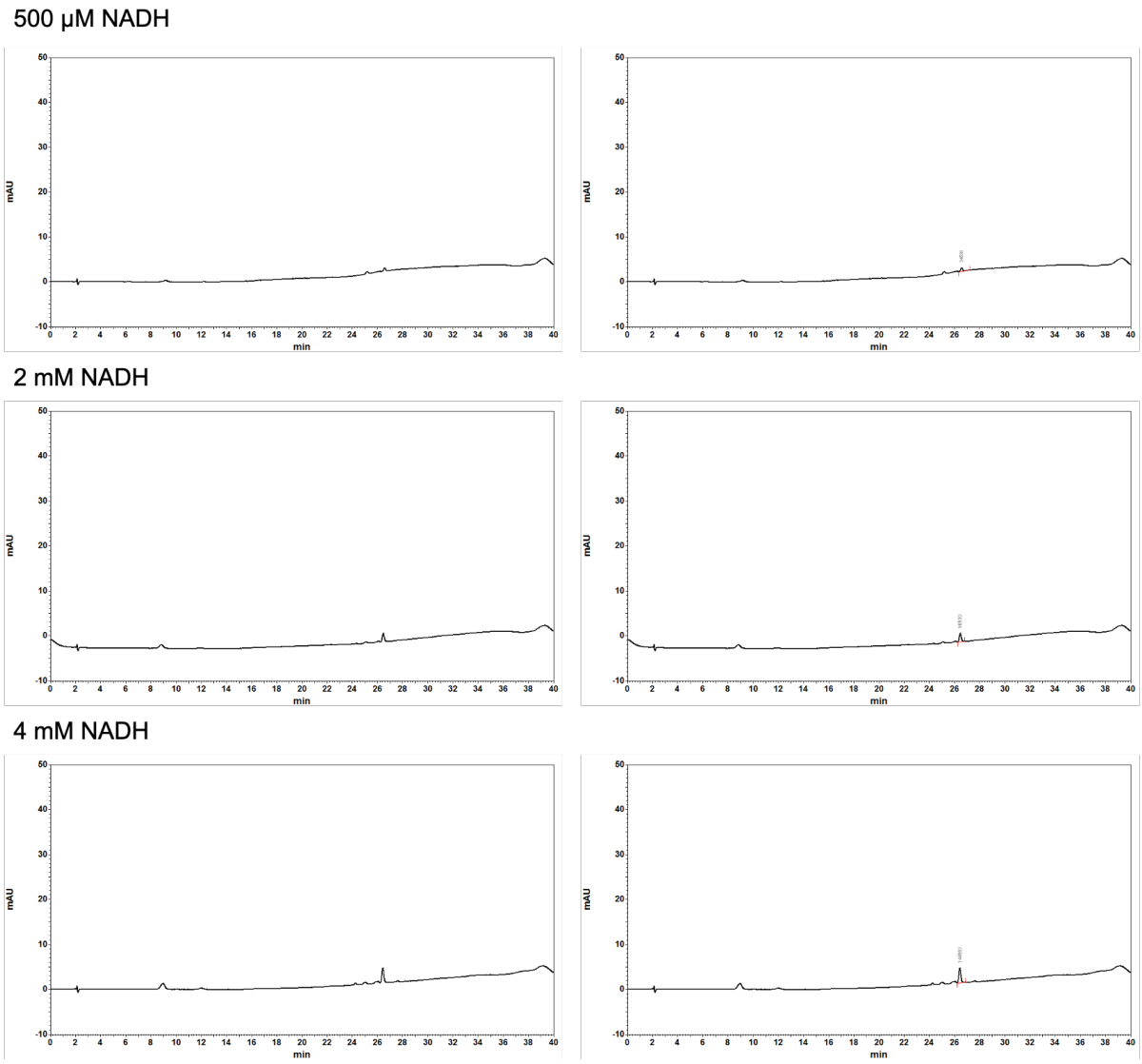

Figure S22. The HPLC chromatograms of LWSO-RD at different NADH concentrations show that NADH was successfully encapsulated in the liposomes. The presence of a distinct NADH peak confirms its retention and encapsulation. Variations in peak intensity correlate with initial NADH concentrations, indicating the effective incorporation of different amounts of NADH into the liposome.

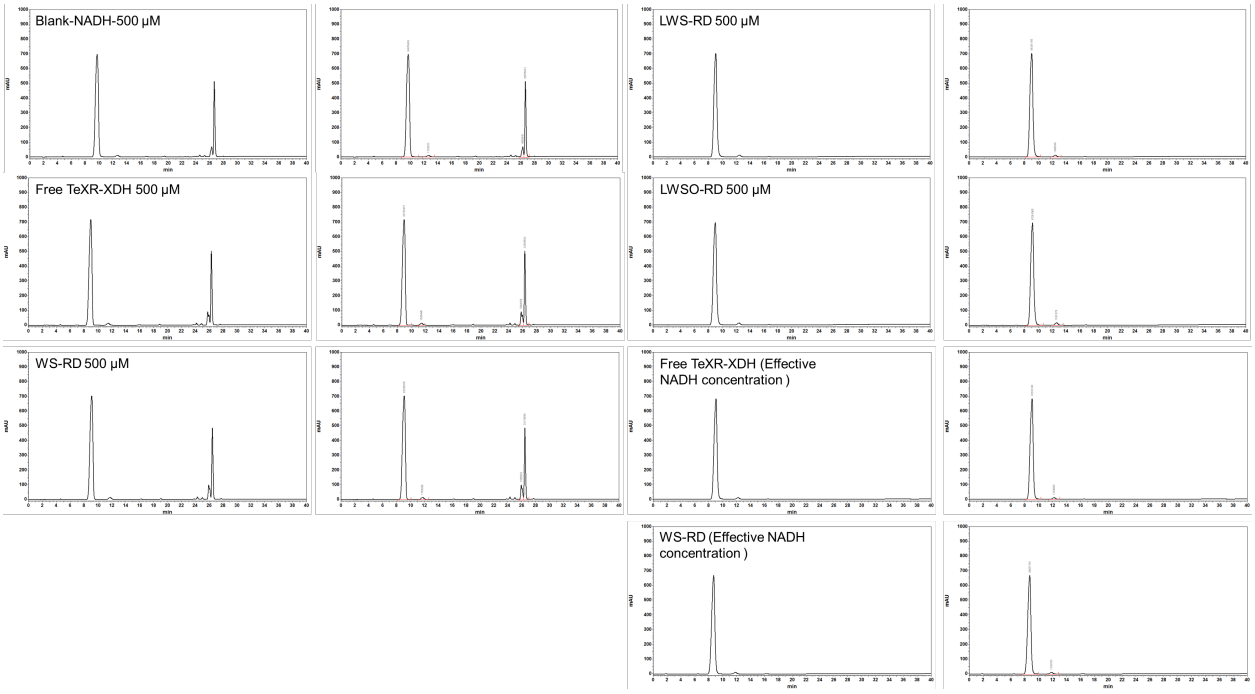

Figure S23. The HPLC chromatographs show the reaction products of Blank (no enzyme), Free TeXR-XDH, WS-RD, LWS-RD, LWSO-RD, and a comparison of actual quantities of 500 μM NADH.

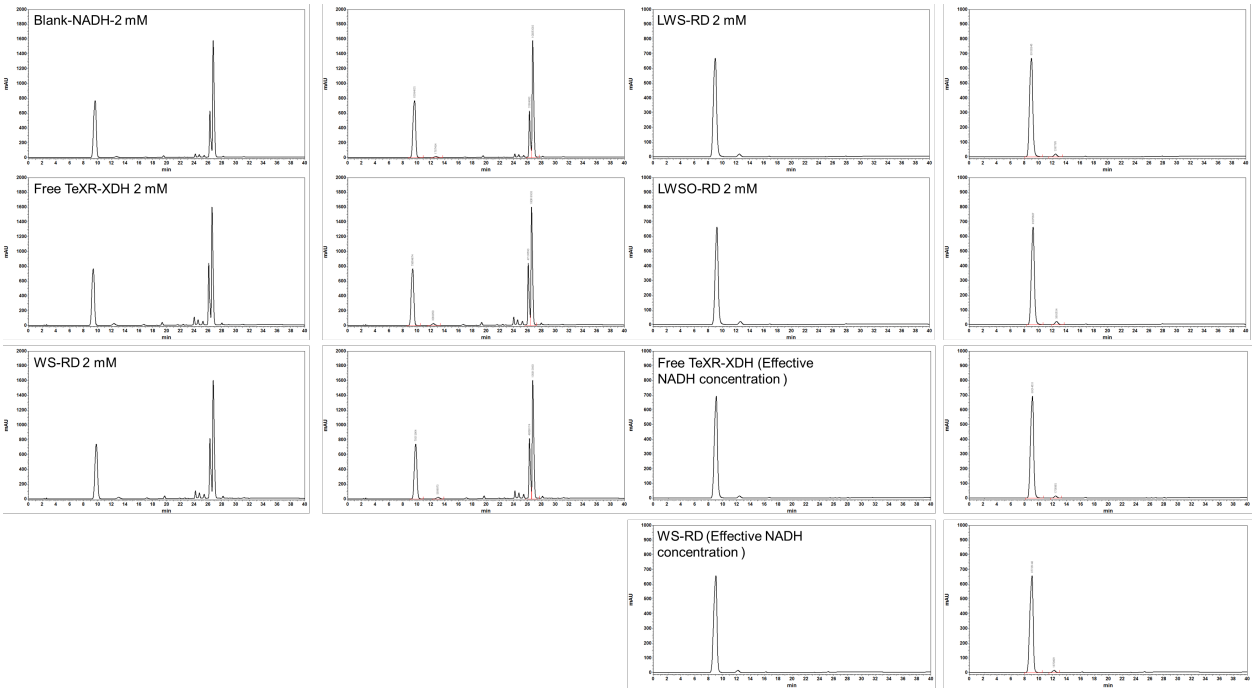

Figure S24. The HPLC chromatograms show the reaction products of Blank (no enzyme), Free TeXR-XDH, WS-RD, LWS-RD, LWSO-RD, and a comparison of actual quantities of 2 mM NADH.

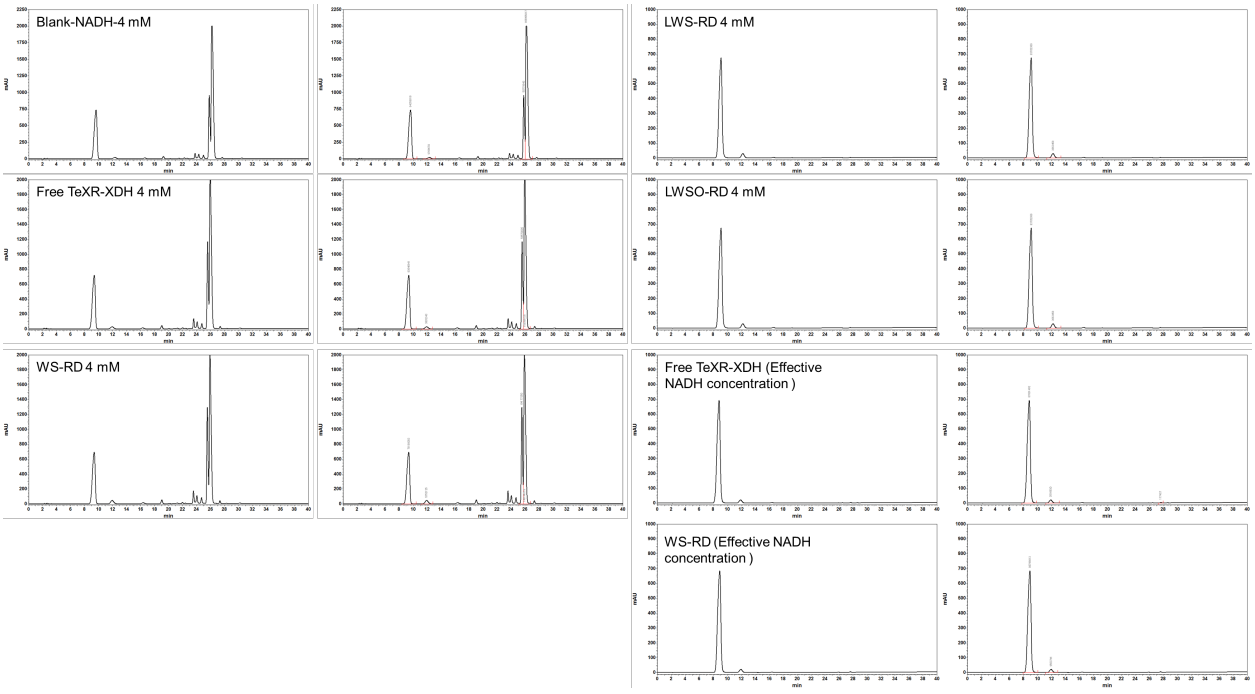

Figure S25. The HPLC chromatograms show the reaction products of Blank (no enzyme), Free TeXR-XDH, WS-RD, LWS-RD, LWSO-RD, and a comparison of actual quantities of 4 mM NADH.

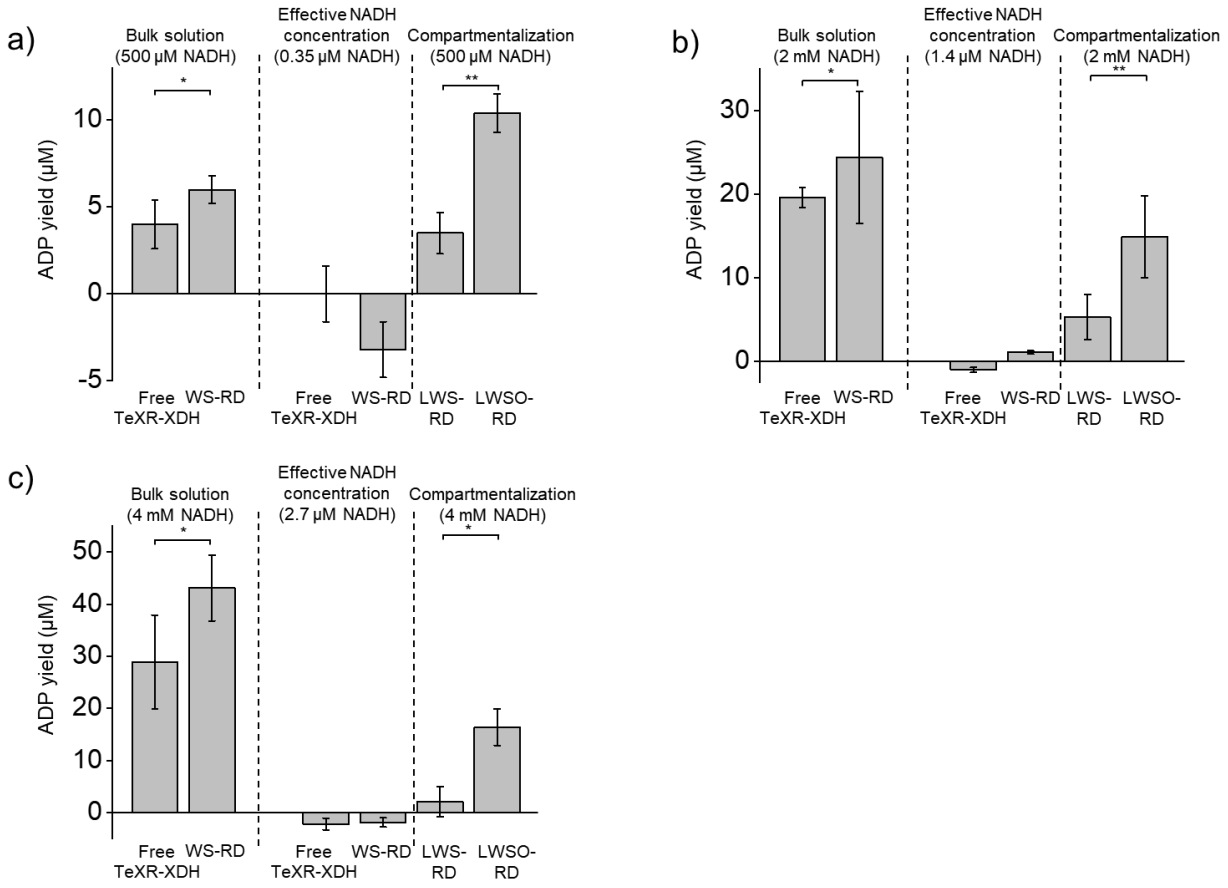

Figure S26. ADP production (μM) of the free enzyme cascade reactions (free TeXR-XDH), the enzyme cascade reactions on the DNA scaffold (WS-RD), and the enzyme cascade reactions on the liposome-coated DNA scaffold (LWS-RD and LWSO-RD). The reactions were carried out with different concentrations of NADH: (a) 500 μM, (b) 2 mM, and (c) 4 mM. Then the products were quantified by HPLC. Asterisks indicate significant difference between groups (*$p < 0.05$ and **$p < 0.01$).

Supplementary References:

1 Zhang, S., Nakata, E., Lin, P. and Morii, T., *Chem.-Eur. J.*, 2023, **29**, e202302093.

2 Zhang, S., Lin, P., Komatsubara, F., Nakata, E. and Morii, T., *ChemBioChem* 2025, **26**, e202401041.